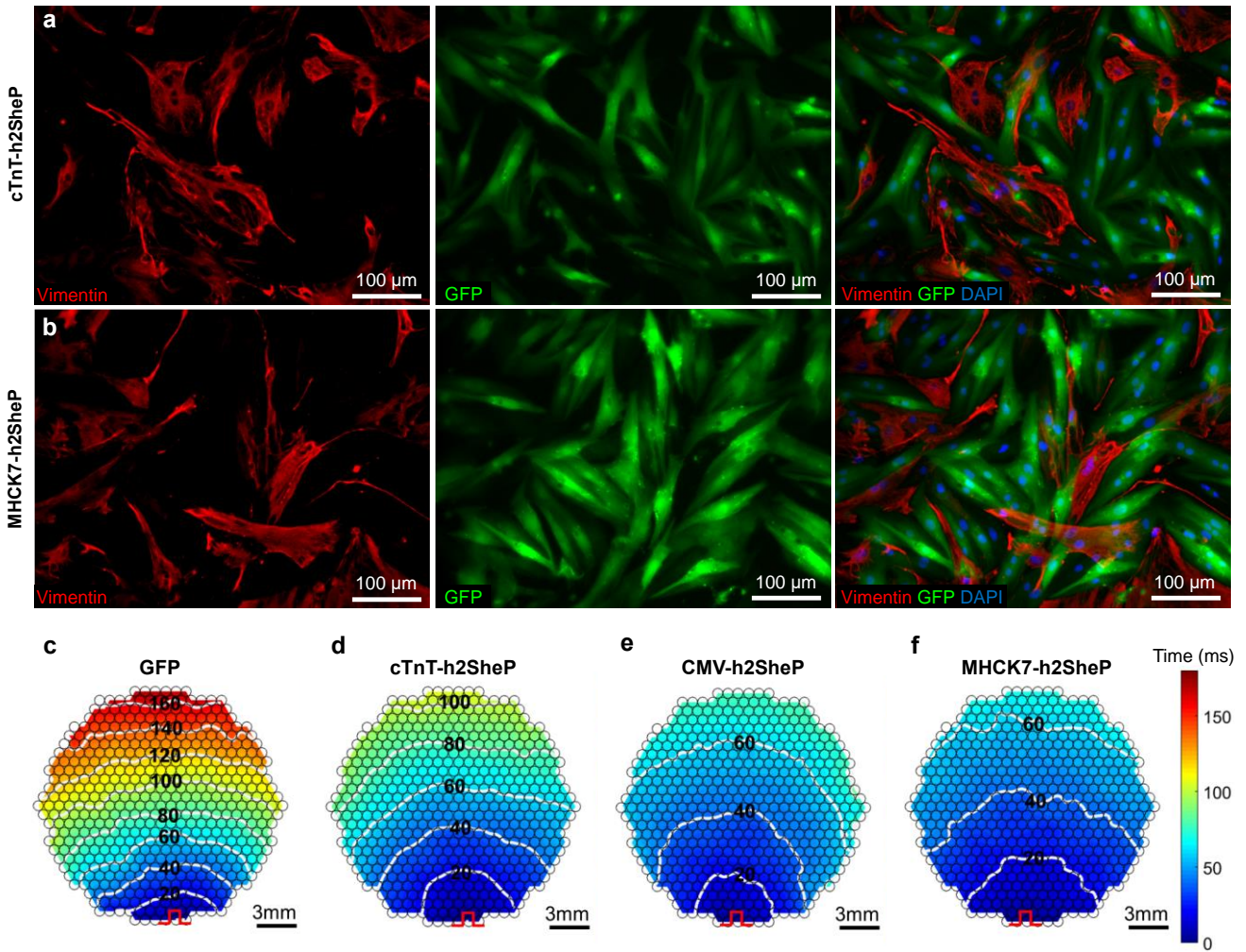
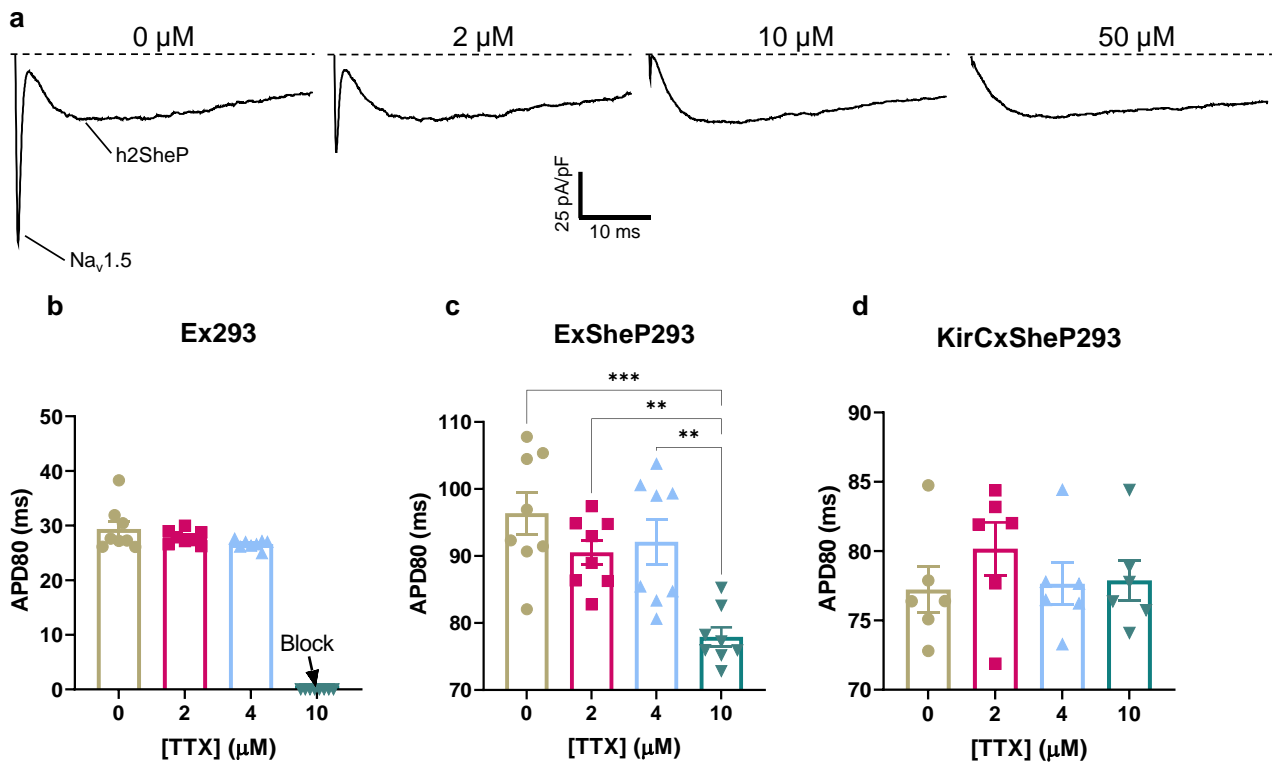


1 **Supplementary Figures**



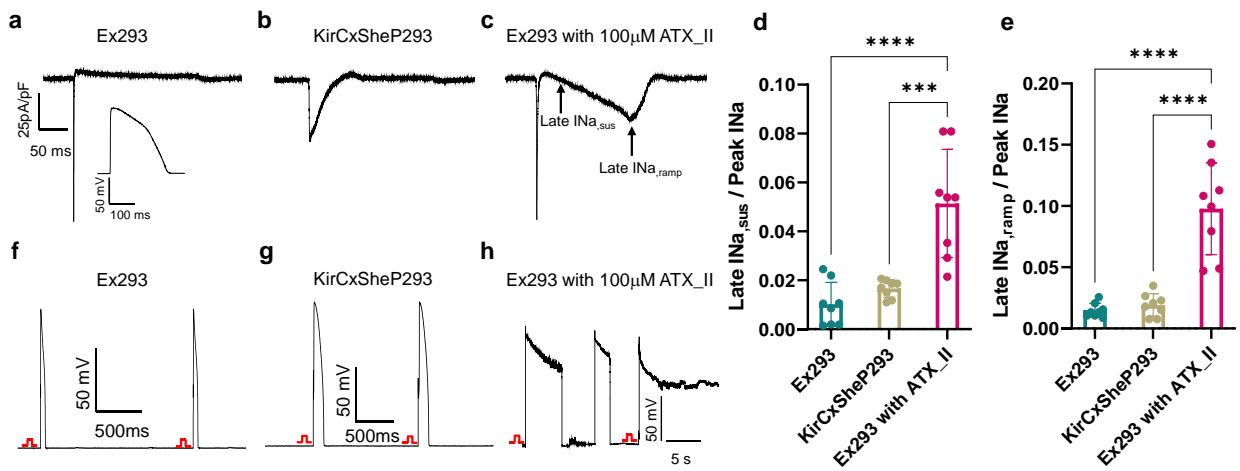
2  
3  
4  
5 **Supplementary Fig. 1: Optimized BacNav expression improves cardiac AP conduction in NRVM**  
6 **monolayers.** **a,b** Representative images of cocultured NRVM-fibroblast monolayers transduced with  
7 cTnT-h2SheP-2A-GFP (**a**) and MHCK7-h2SheP-2A-GFP (**b**) lentiviruses showing that Vimentin<sup>+</sup>  
8 fibroblasts did not express GFP. **c-f**, Representative isochrone activation maps of optically recorded  
9 AP conduction in cocultured NRVM monolayers transduced with lentiviruses expressing GFP (**c**),  
10 cTnT-h2SheP-2A-GFP (**d**), CMV-h2SheP-2A-GFP (**e**), and MHCK7-h2SheP-2A-GFP (**f**). Pulse signs  
11 indicate locations of stimulating electrodes. Circles denote 504 recording sites. Results of quantitative  
12 analysis of AP conduction are shown in Fig. 2.  
13

14  
15  
16  
17  
18  
19  
20  
21  
22



23  
24  
25  
26  
27  
28  
29  
30  
31  
32  
33  
34  
35  
36  
37  
38  
39  
40  
41  
42  
43  
44  
45  
46  
47  
48  
49  
50  
51

**Supplementary Fig. 2: TTX inhibits endogenous Na<sub>v</sub>1.5 but not BacNa<sub>v</sub> current in engineered HEK293 cells.** **a**, Representative voltage-clamp recordings after stepping membrane potential from -80 mV (holding potential) to 0 mV in ExSheP293 cells expressing K<sub>ir</sub>2.1, Cx43, Na<sub>v</sub>1.5, and h2SheP, showing reduced Na<sub>v</sub>1.5 current with increasing TTX concentrations but no change in h2SheP current. Dashed line denotes zero current level. **b-d**, Effects of increasing TTX concentrations on APD<sub>80</sub> of Ex293 (**b**, n = 8; expressing K<sub>ir</sub>2.1, Cx43, Na<sub>v</sub>1.5), ExSheP293 (**c**, n = 8), and KirCxSheP293 (**d**, n = 6; expressing K<sub>ir</sub>2.1, Cx43, and h2SheP) cell lines (for other parameters see Fig. 3). \*\*P=0.0028, 4  $\mu\text{M}$  vs. 10  $\mu\text{M}$  group; \*\*P=0.0085, 2  $\mu\text{M}$  vs. 10  $\mu\text{M}$  group; \*\*\*P=0.0001, 0  $\mu\text{M}$  vs. 10  $\mu\text{M}$  group in **c**. Error bars indicate s.e.m; statistical significance was determined by one-way ANOVA, followed by Tukey's post-hoc test to calculate P values. Source data are provided as a Source Data file.



52

53

54

55

56

57

58

59

60

61

62

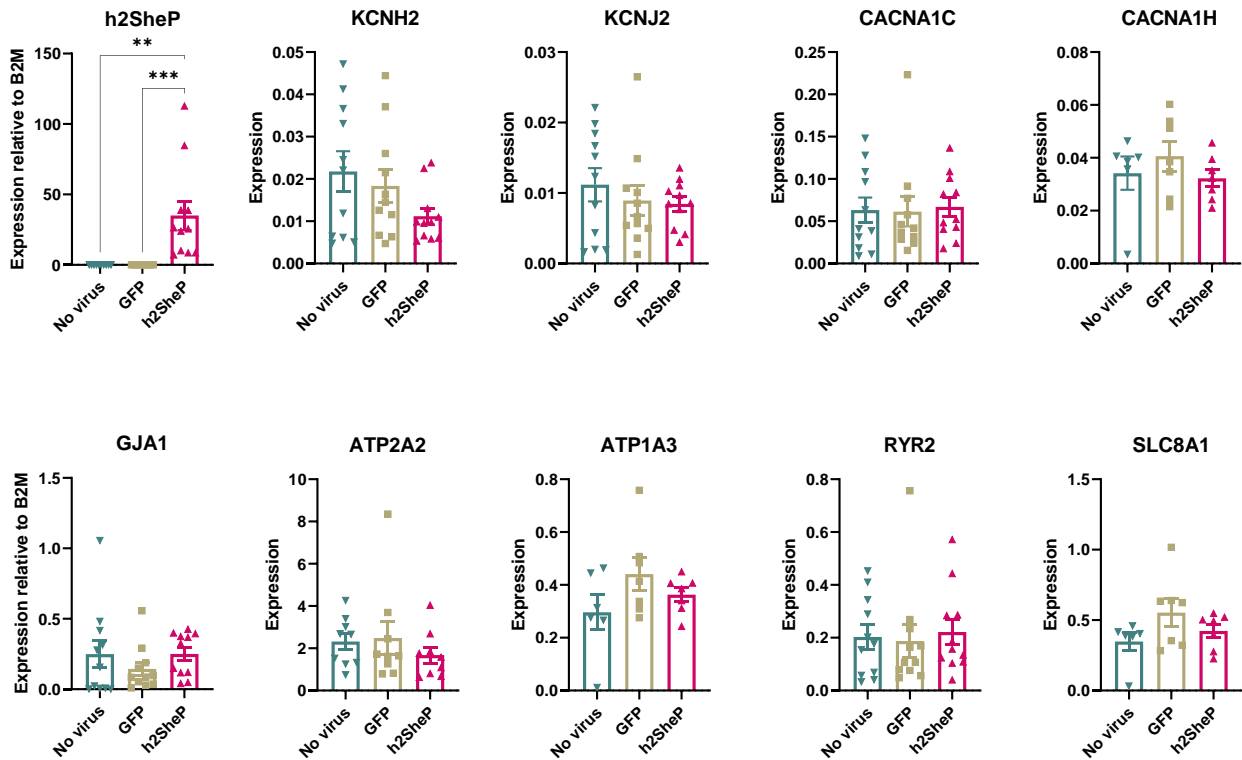
63

64

65

66

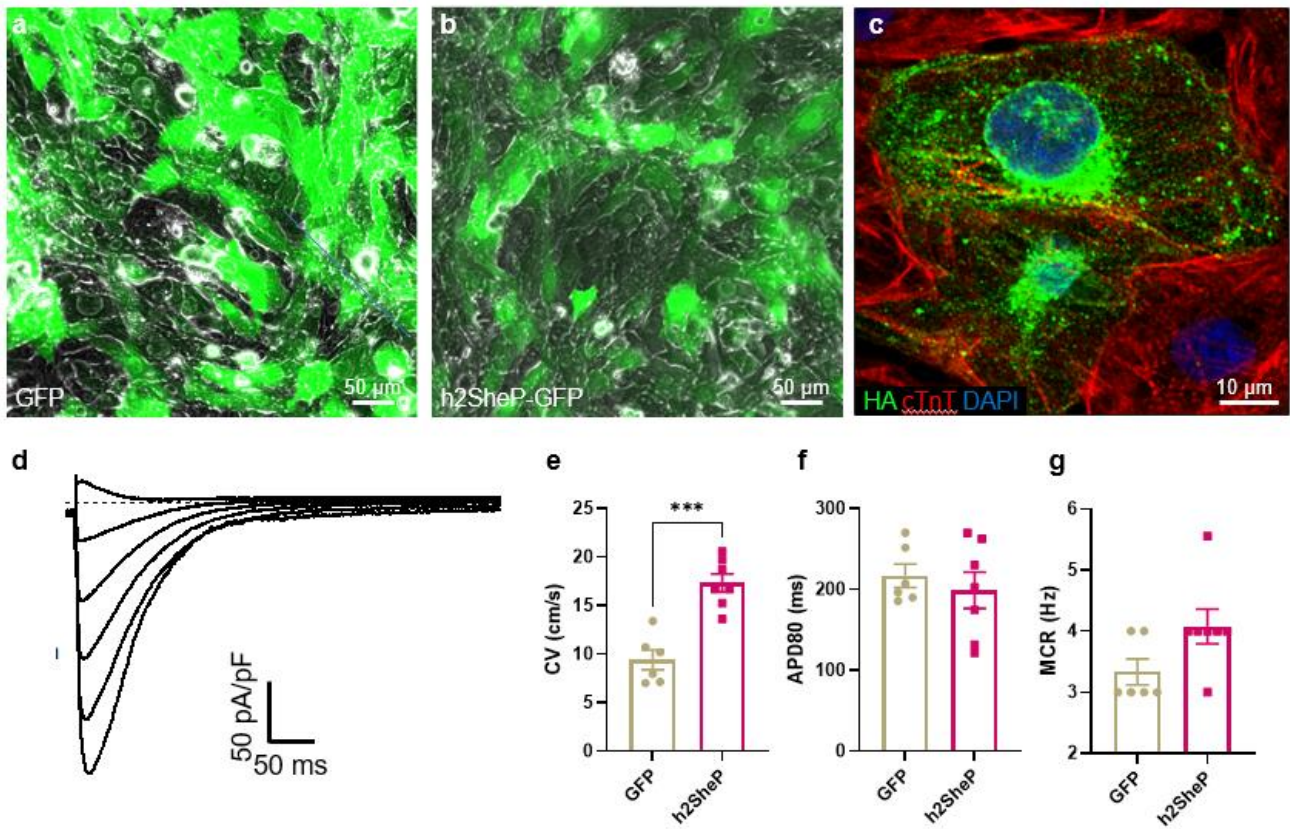
**Supplementary Fig. 3: BacNav current is distinct from ATX II induced late Nav1.5 current.** a-c, Representative Na current ( $I_{Na}$ ) traces recorded during application of a modeled human AP in the AP-clamp, voltage-clamp mode in Nav1.5-expressing Ex293 cells (a), BacNav-expressing KirCxSheP293 cells (b), and Ex293 cells treated with 100  $\mu$ M ATX II (c). Recordings were performed at 25°C in presence of 1mM BaCl<sub>2</sub>. d,e Corresponding quantifications from a-c) of late  $I_{Na,sus}$  measured at 100ms after the onset of AP (d) and late  $I_{Na,ramp}$  measured as maximum late  $I_{Na}$  during AP repolarization (e) \*\*\*\*P=0.0002; \*\*\*\*P<0.0001. n=8 per group. f-h, Representative AP traces recorded via current clamp in Ex293 cells (f), KirCxSheP293 cells (g) and Ex293 cells treated with 100  $\mu$ M ATX II (h). Red pulse signs indicate time of current stimulation. Error bars indicate s.e.m; statistical significance in d,e was determined by one-way ANOVA, followed by Tukey's post-hoc test to calculate P values. Source data are provided as a Source Data file.



67  
68

69 **Supplementary Fig. 4: Stable expression of BacNav<sub>v</sub> in NRVMs does not alter expression of**  
70 **endogenous cardiac ion channel and transporter genes.** All mRNA expression levels for specified  
71 genes are normalized to expression level of B2M housekeeping gene. n=7 biologically independent  
72 samples for ATP1A3, CACNA1H and SLC8A1 expression, n=9 biologically independent samples for  
73 ATP2A2 expression and n=11 biologically independent samples for h2SheP, KCNH2, KCNJ2, RYR2,  
74 CACNA1C and GJA1 expression. \*\*P=0.0011, \*\*\*P=0.0009 vs. h2SheP group for h2SheP  
75 expression. Error bars indicate s.e.m; statistical significance was determined by one-way ANOVA,  
76 followed by Tukey's post-hoc test to calculate P values. Source data are provided as a Source Data file.

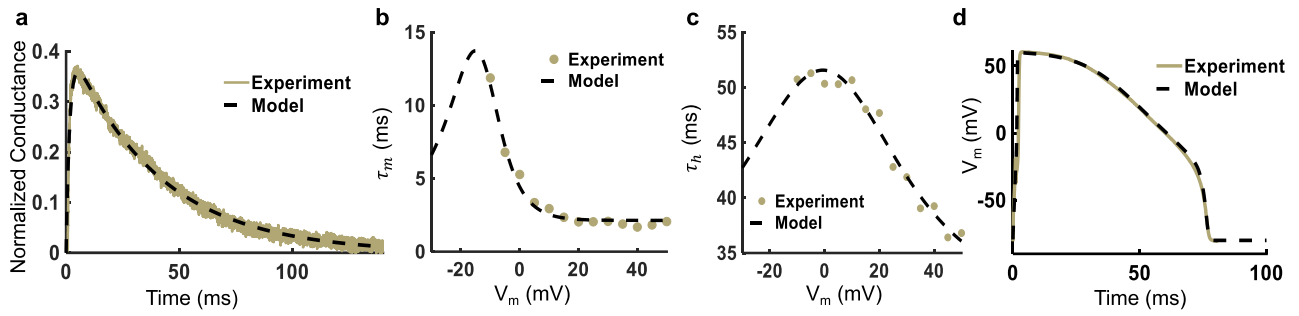
77  
78  
79  
80  
81  
82  
83  
84  
85  
86  
87  
88  
89  
90  
91  
92  
93  
94  
95  
96  
97



98  
99

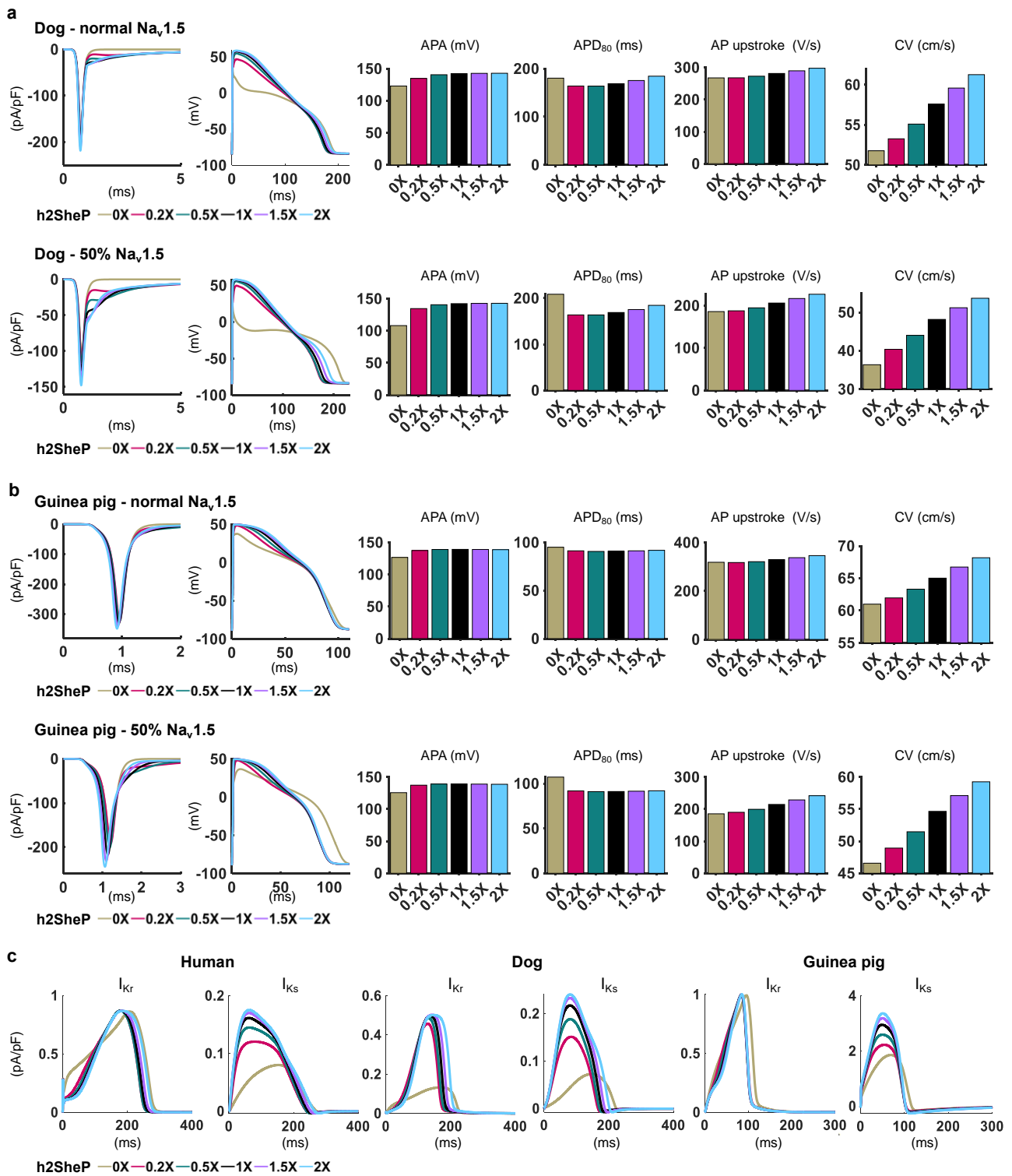
100 **Supplementary Fig. 5: BacNav expression improves AP conduction in hiPSC-CM monolayers.**  
 101 **a,b**, Representative images of hiPSC-CMs transduced with CMV-GFP (**a**) or MHCK7-h2SheP-2A-  
 102 GFP (**b**) lentiviruses. **c**, Representative image of hiPSC-CMs transduced with CMV-h2SheP-HA  
 103 lentivirus showing efficient channel trafficking to membrane. **d**, Representative voltage-clamp  
 104 recordings of sodium current in response to steps of membrane voltages from -80 mV (holding  
 105 potential) to -10 to +40 mV in hiPSC-CMs transduced with CMV-h2SheP-HA lentivirus. Slow kinetics  
 106 of Na current inactivation demonstrates the existence of robust BacNav current. **e-g**, Quantifications  
 107 of CV (**e**), APD<sub>80</sub> (**f**) and MCR (**g**) during AP propagation optically recorded in hiPSC-CM monolayers  
 108 transduced with MHCK7-h2SheP-2A-GFP (“h2SheP”, n = 7) or control MHCK7-GFP (“GFP”, n = 6)  
 109 lentivirus. \*\*\*P=0.0001 versus GFP group in **e**. Error bars indicate s.e.m; statistical significance was  
 110 determined by an unpaired two-tailed Student’s t-test to calculate P values. Source data are provided  
 111 as a Source Data file.

112  
113  
114  
115  
116  
117  
118  
119  
120  
121  
122  
123  
124  
125  
126



127  
 128  
 129  
 130  
 131  
 132  
 133  
 134  
 135  
 136  
 137  
 138  
 139  
 140  
 141  
 142  
 143  
 144  
 145  
 146  
 147  
 148  
 149  
 150  
 151  
 152  
 153  
 154  
 155  
 156  
 157  
 158  
 159  
 160  
 161  
 162  
 163  
 164  
 165  
 166  
 167

**Supplementary Fig. 6: Optimized computational model of BacNav channel shows excellent agreement with experimental results.** **a**, Representative experimental and simulated traces of normalized h2SheP conductance during voltage-clamp step from -80mV to -10 mV. **b,c**, Time constants of activation (**b**) and inactivation (**c**) extracted from experimental data and corresponding curves generated from the simulations using optimized BacNav model. **d**, Representative patch-clamp AP recording of HEK293 cell expressing  $K_{ir2.1}$  and h2SheP and corresponding model-fit trace. Note excellent agreement between experimental and simulated data.



168

169

170

171

172

173

174

175

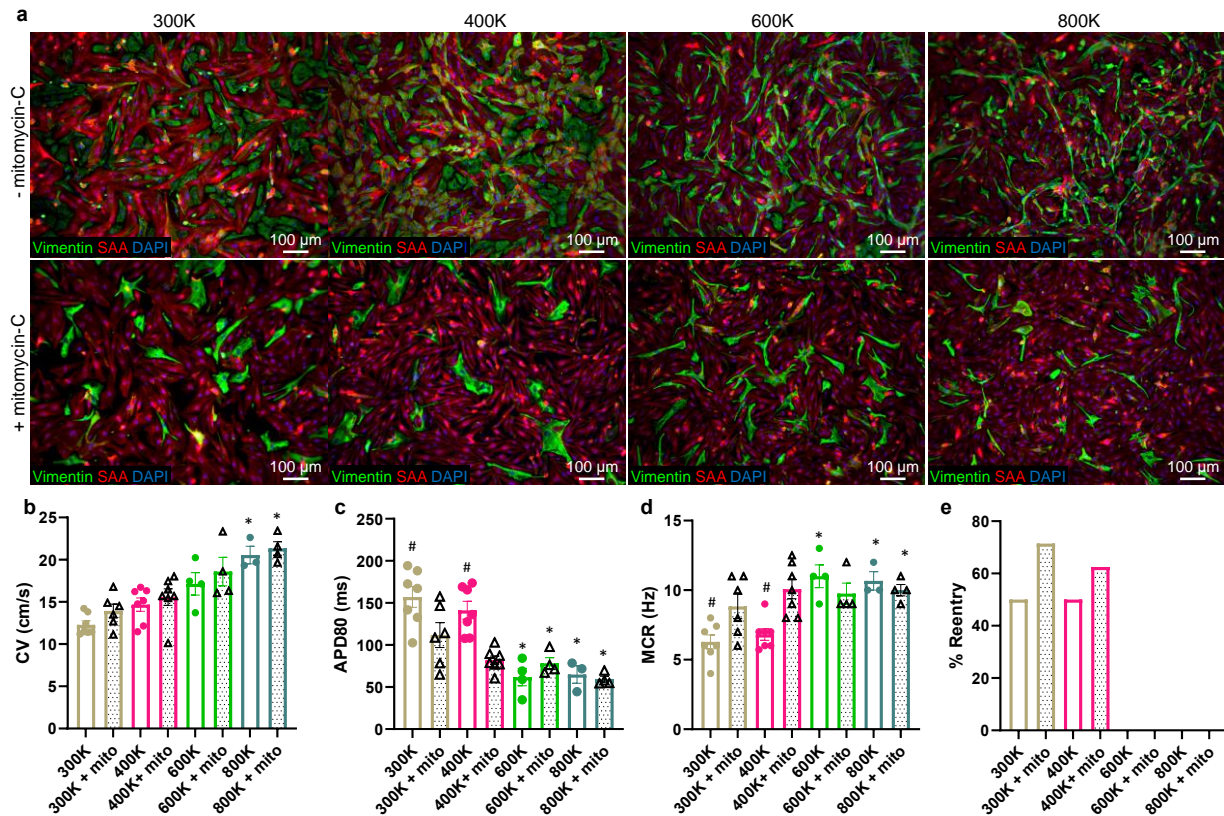
176

177

178

179

**Supplementary Fig. 7: Simulated h2SheP expression results in increased excitability, improved AP conduction, and augmented  $I_{Ks}$  in computational models of adult ventricular myocytes. a,b,** Simulated effects of various h2SheP expression levels (0X to 2X) on total sodium current, AP shape, amplitude (APA), duration ( $\text{APD}_{80}$ ), and maximum upstroke velocity (AP upstroke), and conduction velocity (CV) in adult dog (a) and guinea pig (b) ventricular myocyte models under normal and reduced (50% of normal  $\text{Na}_v1.5$  current) excitability. c, Simulated effects of various h2SheP expression levels (0X to 2X) on  $I_{K_r}$  and  $I_{K_s}$  currents shown during human, dog, and guinea pig ventricular myocyte APs.



180

181

182

183

184

185

186

187

188

189

190

191

192

193

194

195

196

197

198

199

200

201

202

203

204

205

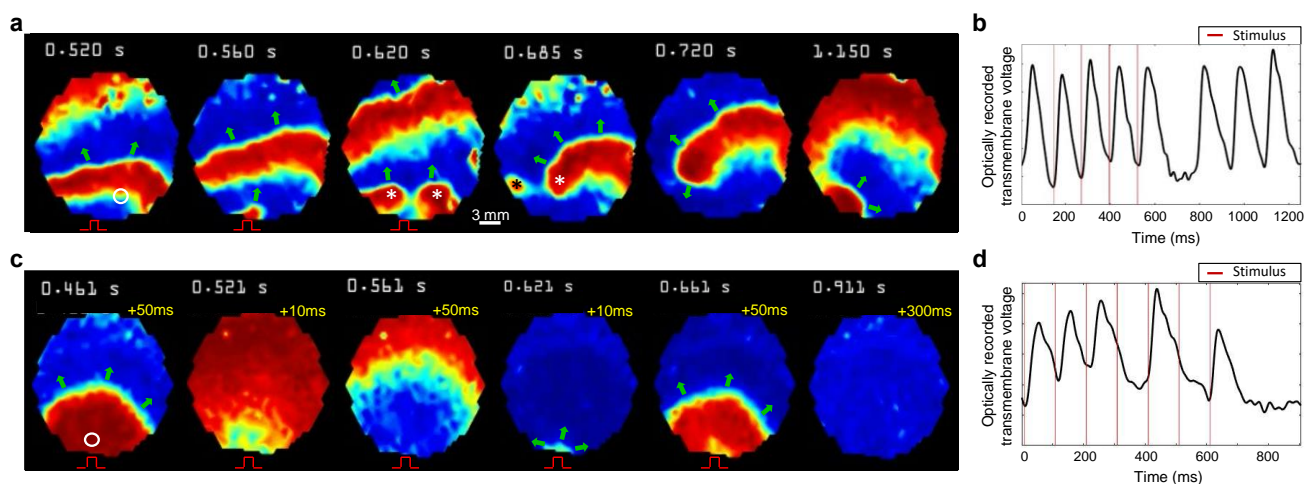
206

207

208

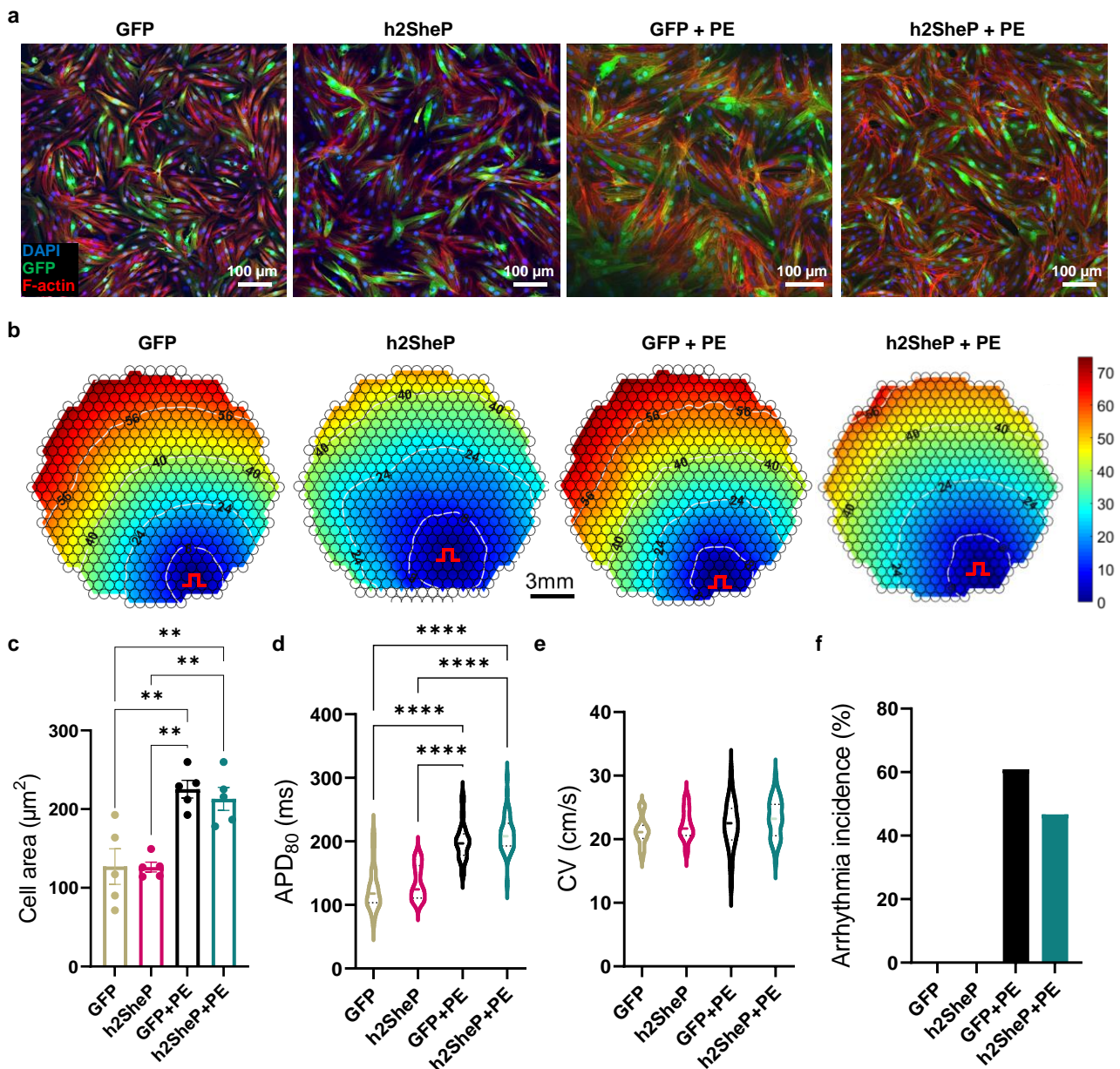
**Supplementary Fig. 8: Varying cell seeding density and treatment with mitomycin-C yield highly arrhythmogenic NRVM cultures.** **a**, Representative immunostaining images of NRVM cultures with varying cell seeding densities (from 300-800K cells per well of a 12-well plate), with and without mitomycin-C treatment. Increasing cell seeding density led to a higher content of vimentin<sup>+</sup> fibroblasts at intermediate densities (400K) and changes in fibroblast morphology at higher densities (600K and 800K), while mitomycin-C treatment effectively reduced fibroblast content in all conditions. **b-d**, Effects of cell seeding density and mitomycin-C treatment (+mito) on CV (**b**), APD<sub>80</sub> (**c**), and MCR (**d**) of NRVM monolayers (n = 3, 800k; n = 4, 600k, 600k+mito, 800k+mito; n = 6, 300k+mito; n = 7, 300k, 400k, 400k+mito). **e**, Incidence of reentry in NRVM cultures was significantly more prevalent at lower cell seeding densities and further increased with mitomycin-C treatment. \*P<0.05 from both 300K and 400K groups and #P<0.05 vs. corresponding +mito group. Exact P values for all comparisons are included in **Source Data**. Error bars indicate s.e.m; statistical significance was determined by two-way ANOVA, followed by Tukey's post-hoc test to calculate P values. Source data are provided as a Source Data file.





209  
210  
211  
212  
213  
214  
215  
216  
217  
218  
219  
220  
221  
222  
223  
224  
225  
226  
227  
228  
229  
230  
231  
232  
233  
234  
235

**Supplementary Fig. 9: BacNav expression in arrhythmogenic NRVM monolayers prevents induction of reentrant activity.** **a**, Representative movie snapshots of optically recorded membrane potentials in arrhythmogenic NRVM monolayers transduced with control MHCK7-GFP lentivirus, shown during rapid point pacing which yielded reentry induction (see also Supplementary Movie 3). Rapid pacing (8 Hz) from the bottom of the monolayer generated a wave break and two transiently coexisting waves (white asterisks) distal to the pacing site, one which was annihilated against the tissue boundary (black asterisk) and another which continued to stably rotate after pacing was terminated. **b**, Representative membrane voltage trace optically recorded from the specified monolayer site (white circle) in **a**, showing the pacing-induced (red lines) action potentials, followed by self-sustained activity due to reentry. **c**, Representative snapshots of optically recorded membrane voltage shown during rapid pacing in arrhythmogenic NRVM monolayers transduced with MHCK7-h2SheP-2A-GFP lentivirus (see also Supplementary Movie 3). Rapid pacing (10 Hz) from the bottom of the monolayer did not result in the formation of distal wave break, but rather induced a proximal conduction block at the pacing site, every other beat (1:2 conduction). In **a,c**, elapsed time (in seconds) since the beginning of recording is shown in white font above the voltage snapshot. Blue and red color in snapshots indicate resting and activated tissue, respectively. Green arrows denote directions of the propagating wave fronts. Pulse signs indicate locations of stimulus electrode. The lack of pulse sign denotes that pacing was terminated. Numbers in ms in **c** specify time elapsed from the last paced stimulus; the stimulus delivered at 0.511 s did not elicit AP propagation (as evident from no new launched wave at 0.521 s and 0.561 s snapshots). **d**, Representative membrane voltage trace optically recorded from the specified monolayer site (white circle) in **c**, showing the initial 1:1 tissue capture, followed by the partial capture of every other pacing-induced AP, and eventually cessation of all activity after pacing is terminated, thus not resulting in reentry induction. In **b,d**, red lines denote times when pacing stimuli were delivered.



236

237

238

239

240

241

242

243

244

245

246

247

248

249

250

251

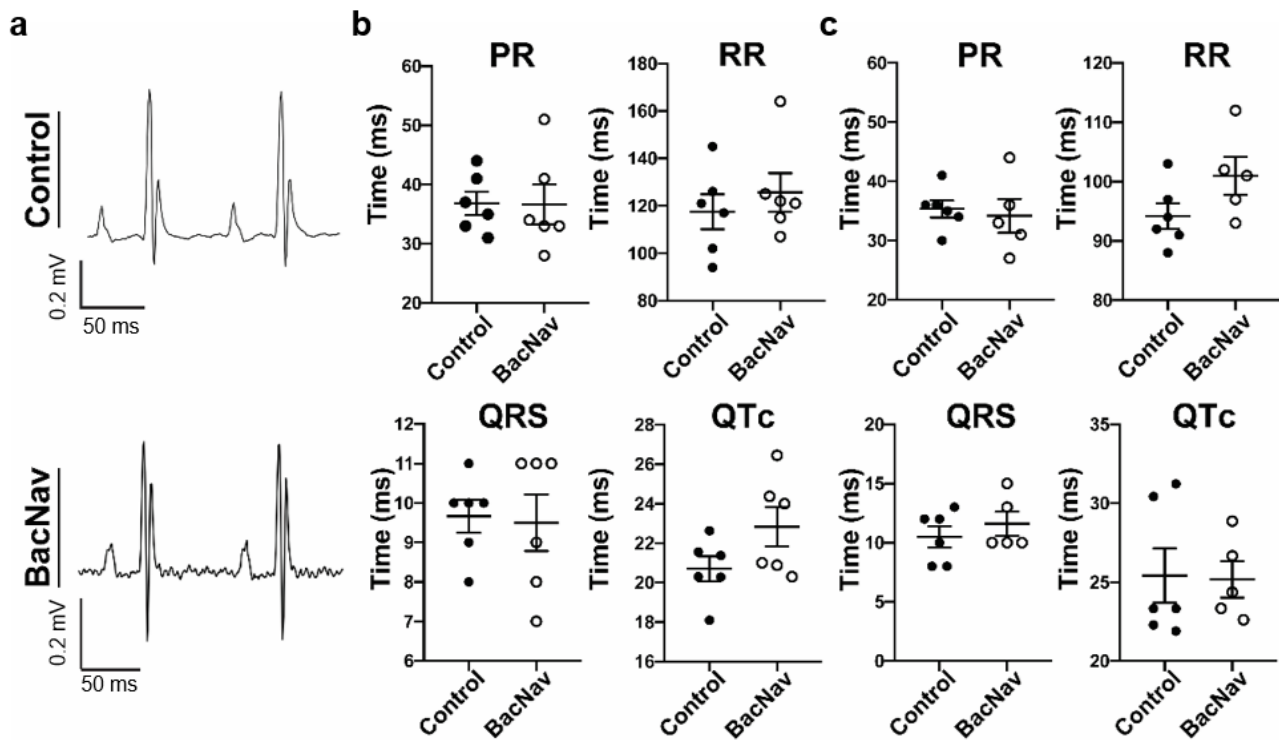
252

253

254

**Supplementary Fig. 10: BacNav expression in phenylephrine-treated NRVM monolayers does not decrease incidence of triggered activity.** **a**, Representative immunostaining images of NRVM monolayers transduced with control MHCK7-GFP (“GFP”) or MHCK7-h2SheP-2A-GFP (“h2SheP”) lentivirus, showing larger cell size in the phenylephrine (PE) treated groups. **b**, Representative isochrone activation maps of AP propagation in non-treated or PE-treated (“+PE”) NRVM monolayers transduced with specified lentivirus. Pulse signs indicate location of pacing electrode and circles denote 504 recording sites. **c-e**, Cell area (**c**,  $n=5$ ,  $**P=0.0013$ , GFP vs. GFP+PE;  $**P=0.0044$ , GFP vs. h2SheP+PE;  $**P=0.0013$ , h2SheP vs. GFP+PE;  $**P=0.0041$ , h2SheP vs. h2SheP+PE), AP duration ( $APD_{80}$ , **d**,  $****P<0.0001$ ), conduction velocity (CV, **e**), and incidence of triggered activity (**f**, see also Supplementary Movie 4) in the four monolayer groups. Phenylephrine treatment in GFP+PE ( $n=46$ ) and h2SheP+PE ( $n=45$ ) monolayers resulted in increased cell area,  $APD_{80}$ , and arrhythmia incidence, but not CV, compared to untreated GFP ( $n=24$ ) or h2SheP ( $n=24$ ) monolayers. h2SheP expression did not significantly decrease incidence of triggered activity induced by PE ( $P=0.1742$ ). Error bars indicate s.e.m; statistical significance in **c-e** was determined by one-way ANOVA, followed by Tukey’s post-hoc test to calculate P values; statistical significance in **f** was determined by two-sided Chi square test. Source data are provided as a Source Data file.

254



255  
256

257 **Supplementary Fig. 11: Intravenous AAV-mediated delivery of BacNav does not alter cardiac**  
 258 **electrophysiology in healthy mice.** **a**, Representative surface ECG traces in mice six weeks after  
 259 injection of  $1 \times 10^{12}$  vg of scAAV-MHCK7-GFP (Control) or scAAV-MHCK7-h2SheP-HA (BacNav).  
 260 **b-c**, ECG parameters in control (n=6) and BacNav (n=5) groups measured before (**b**) and after (**c**)  
 261 administration of 200 $\mu$ g/g caffeine and 1 $\mu$ g/g isoproterenol. Error bars indicate s.e.m. PR, PR-interval  
 262 duration; RR, RR-interval duration; QRS, QRS-complex duration; QTc, corrected QT-interval  
 263 duration. Source data are provided as a Source Data file.

264  
265  
266  
267

268  
269  
270  
271

**Supplementary Table 1: List of qPCR primers.** All rat primers (B2M as house-keeping gene) were used for studies of NRVM genes. All human primers (GAPDH as house-keeping gene) were used for studies of HEK293 genes.

Gene	Description	Species	Forward Primer	Reverse Primer
ATP1A3	Na <sup>+</sup> /K <sup>+</sup> ATPase alpha 3	Rat	CTGTCATCTTCC TCATCGGTATC	GACAGTTCTTC CGAGCCAT
ATP2A2	SERCA-2a	Rat	TGTGCTCTGTGT AATGACTCTG	CTCCGTGTCGA ATACATTCATC T
B2M	Beta-2 Microglobulin	Rat	GCTTGCAGAGT TAAACACGTC	CCAGATGATTC AGAGCTCCAT
CACNA1C	L-type Ca Channel (Ca <sub>v</sub> 1.2)	Rat	ACTTCATCATCC TCTTCATCTGTG	CCAGCTTCTTT CTCTCCTTCTC
CACNA1H	T-type Ca Channel (Ca <sub>v</sub> 3.2)	Rat	CACTCGTTCTAC AACTTCATCTAC T	CTCTGAGAACT GTGTGGCTATC
GAPDH	Glyceraldehyde-3-phosphate dehydrogenase	Human	AAGGTGAAGGT CGGAGTCAA	ATGAAGGGGTC ATTGATGG
GJA1	Gap junction protein α-1 (Connexin 43)	Rat	GAGCTGTCGAT TATGGAGGA	AGGTTCAGTTG GGGGATG
h2SheP	Bacteria voltage-gated Na channel	Rat	CCTTACGCCTGG GTGTTCTT	CAGCGCATGTT CTTCATCGG
KCNH2	Voltage-gated inwardly rectifying potassium channel (K <sub>v</sub> 11.1)	Rat	CAGTGACCGGG AAATCATAGC	ACATTGTGGGT CCGCTCTTT
KCNJ2	Inward-rectifier potassium channel (K <sub>ir</sub> 2.1)	Rat	GTGTCTGAGGT CAACAGCTT	GAAACCATAGC CGATGGTTG
KCNJ2	Inward-rectifier potassium channel (K <sub>ir</sub> 2.1)	Human	TGTCACGGATG AATGCCAA	CTGCGCCAATG ATGAAAGCA
RYR2	Ryanodine receptor 2	Rat	GCAGTTGATTG AGCCTAGTGT	CCTCTTTGACT TCCAGTTTAGA GT
SCN5A	Voltage-gated Na channel (Na <sub>v</sub> 1.5)	Rat	CGTAACTTCACC GAGCTCAA	CCCACATAGTA ACACATCCGT
SCN5A	Voltage-gated Na channel (Na <sub>v</sub> 1.5)	Human	TTCAGGGCTGA AGACCATCG	GCACTTGTGCC TTAGGTTGC
SLC8A1	Sodium/calcium exchanger	Rat	CCTATAAAACC ATTGAAG GCACAG	TTTTCTCATACT CCTCGTCATCG

272  
273  
274  
275  
276  
277  
278

279 **Supplementary Methods:**

280 **Wild-type and codon-optimized sequences of NavSheP D60A**

281 bSheP:

282 ATGAGTACATCTTTACTTAACGCGCCAACGGGTTTGCAGGCACGAGTGATTAACCTGGT  
283 TGAGCAAAACTGGTTTGGTCATTTTATTTTGGCATTGATTTTAATCAACGCGGTGCAGTT  
284 AGGTATGGAGACCTCAGCCAGCCTGATGGCGCAATACGGTACTTTGTTGATGAGTCTTG  
285 ATAAGTTGCTACTGAGTGTATTTGTGGTGGAGTTATTGCTGCGGATTTATGCCTACAGGG  
286 GGAAATTTTTTAAAGACCCTTGGAGCGTGTTTCGATTTTACCGTGATAGTGATAGCACTGA  
287 TCCCTGCATCTGGGCCATTGGCTGTCTGCGTTCGCTCAGGGTATTGCGGGTGCTGAGAG  
288 TGTTAACAATTGTGCCATCAATGAAACGGGTGGTGTCTGCGCTGTTGGGATCACTTCCTG  
289 GATTGGCATCGATCGCCACGGTATTACTGTTGATTTATTATGTGTTTGCGGTGATTGCTA  
290 CCAAATTTTTGGCGATGCATTCCCTGAATGGTTTGGCACTATTGCTGACTCATTTTATA  
291 CCCTATTTCAAATAATGACGCTTGAAAGCTGGTCTATGGGAATTCGCGGCCAGTGATG  
292 GAAGTGTACCCTTATGCTTGGGTATTTTTCGTACCATTTATTCTGGTAGCGACTTTCACA  
293 ATGCTAAATTTGTTTATTGCGATTATCGTCAATACCATGCAAACCTTCAGCGACGAAGA  
294 GCATGCATTAGAGCGTGAACAAGACAAACAATCTTAGAGCAGGAACAAAGACAAATG  
295 CACGAGGAGTTGAAAGCCATCAGACTCGAGCTACAACAATTACAAACCTTGTTGCGCAA  
296 TGCTGCTGGTGATTCTTCTAATGTGTGCGACAAAGGGAAACATTGGTTCTGACTGA  
297

298 hSheP:

299 ATGTCAACCTCACTGCTGAACGCTCCAACCTGGGCTGCAGGCAAGAGTCATCAATCTGGT  
300 CGAACAGAACTGGTTTGGGCACTTTATTCTGGCACTGATCCTGATTAACGCAGTGCAGC  
301 TGGGAATGGAGACCAGCGCCTCCCTGATGGCACAGTACGGAACACTGCTGATGTCCCTG  
302 GCAAAGCTGCTGCTGAGCGTGTTTCGTGGTTCGAACTGCTGCTGCGAATCTACGCCTATCG  
303 GGGCAAGTTCTTTAAAGACCCCTGGAGCGTGTTTCGACTTCACCGTGATCGTCATTGCCCT  
304 GATTCCAGCTAGTGGACCTCTGGCCGTGCTGCGGTCACTGAGAGTGCTGAGGGTCTGC  
305 GCGTGCTGACAATCGTGCCTAGCATGAAGAGGGTGGTCTCAGCTCTGCTGGGCAGCCTG  
306 CCAGGACTGGCATCCATCGCTACTGTGCTGCTGCTGATCTACTATGTCTTCGCAGTGATC  
307 GCCACTAAAATTTTCGGAGACGCTTTTCCCAGTGGTTCGGCACCATCGCAGATTCTTTT  
308 TATACTGTTCCAGATCATGACTCTGGAGTCTTGGAGTATGGGCATCAGTCGCCCAGT  
309 CATGGAAGTGTACCCCTATGCCTGGGTCTTCTTTGTGCCTTTTATTCTGGTCCGCCACCTT  
310 ACAATGCTGAACCTGTTTATCGCTATCATTGTGAATACTATGCAGACCTTTAGCGACGA  
311 GGAACACGCTCTGGAGCGAGAACAGGATAAGCAGATTCTGGAGCAGGAACAGAGACA  
312 GATGCATGAGGAACTGAAAGCAATCAGGCTGGAGCTGCAGCAGCTGCAGACACTGCTG  
313 AGAAACGCTGCTGGCGATTTCATCAAACGTGTCCACTAAAGGAAACATTGGCTCTGACTG  
314 A  
315

316 h2SheP:

317 ATGTCAACCTCCCTTCTGAACGCCCCCACCAGTCTGCAAGCCCGCGTCATCAACCTGGTC  
318 GAACAGAACTGGTTCGGCCACTTCATCCTCGCACTGATTCTCATTAAACGCCGTGCAGCTT  
319 GGAATGGAACTAGCGCGTCCCTGATGGCTCAATACGGCACACTGCTCATGAGCCTGGC  
320 GAAGCTGCTCCTGTCCGTGTTTCGTGGTGGAACTGTTGCTGCGGATCTATGCGTACCGCG  
321 GAAAATTCTTCAAGGATCCATGGAGCGTGTTTCGACTTTACTGTGATTGTGATCGCACTCA  
322 TCCCGGCCTCGGGACCGCTCGCCGTGCTCCGGTCACTGAGAGTCTTGAGGGTGCTCAGA  
323 GTGCTGACCATTGTGCCTAGCATGAAGCGCGTGGTGTCCGCCCTGTTGGGATCCCTGCC  
324 GGGTTTGGCTTCGATTGCCACTGTGCTGCTCCTGATCTACTACGTGTTTCGCCGTCAATTGC  
325 CACTAAGATTTTCGGCGACGCCTTTCTGAGTGGTTCGGAACCATCGCTGACTCTTTCTA  
326 CACCTTGTTCCAAATCATGACCCTGGAATCCTGGTCCATGGGGATTTTCGAGGCCCGTGA  
327 TGGAGGTGTACCCTTACGCCTGGGTGTTCTTCGTCCCCTTCATCCTTGTGCGAACCTTCA  
328 CCATGCTTAACCTGTTTATCGCCATCATCGTGAACACGATGCAGACCTTCTCCGATGAAG  
329 AACATGCGCTGGAGCGGGAACAGGACAAGCAGATCCTGGAGCAGGAACAGCGGCAGA  
330 TGCACGAGGAGCTGAAGGCCATCCGGCTGGAGCTGCAGCAGCTCCAAACTCTGCTGCGC  
331 AACGCGGCCGGAGATTCAAGCAATGTGTGCGACCAAGGGGAACATCGGCTCCGACTGA

## 332 MATLAB code for computational modeling of NavSheP D60A

333

334 This function takes the current membrane voltage ( $v$ ), maximum BacNav conductivity ( $GNa$ ), an  
335 output switch, and the current values for the gating state variables ( $m$  and  $h$ ). If the output switch is 1,  
336 output is the steady-state conductivity ( $gna$ ), gating state variables ( $minf$ ,  $hinf$ ), and the time constants  
337 for that specific voltage value. If the output switch is 2, output is the conductivity ( $gna$ ), and derivatives  
338 for the state variables ( $dm$ ,  $dh$ ). If used in a cell model,  $gna$  should be multiplied by the driving force  
339 ( $V-E_{Na}$ ) to get BacNav current.  $dm$  and  $dh$  can be used directly with `ode15s` or other solvers, or  
340 multiplied by  $dt$  in an explicit Euler solver.

341

```
342 function [gna, varargout] = bacnav_channel_paper(v, GNa, outswitch, varargin)
```

```
343 if outswitch==2
```

```
344     if nargin==5
```

```
345         m = varargin(1);
```

```
346         h = varargin(2);
```

```
347     else
```

```
348         error('Please enter the correct number of parameters for mh');
```

```
349     end
```

```
350 end
```

351

```
352 minf_v50_mhleg = -28.34;
```

```
353 minf_slope_mhleg = 5.33;
```

```
354 hinf_v50_mhleg = -77.21;
```

```
355 hinf_slope_mhleg = 8.32;
```

```
356 taum_mhleg_a = 86.37;
```

```
357 taum_mhleg_b = -82.74;
```

```
358 taum_mhleg_c = 17.64;
```

```
359 taum_mhleg_d = -6.008;
```

```
360 taum_mhleg_e = 3.337;
```

```
361 taum_mhleg_f = .4844;
```

```
362 tauh_mhleg_a = 96.17;
```

```
363 tauh_mhleg_b = 10.45;
```

```
364 tauh_mhleg_c = -23.26;
```

```
365 tauh_mhleg_d = 2.529;
```

```
366 minf = sigmoid(v, minf_v50_mhleg, minf_slope_mhleg);
```

```
367 hinf = 1-sigmoid(v, hinf_v50_mhleg, hinf_slope_mhleg);
```

```
368 taum = hypsec(v, taum_mhleg_a, taum_mhleg_b, taum_mhleg_c, taum_mhleg_d, taum_mhleg_e,  
369 taum_mhleg_f);
```

```
370 tauh = sigmoid_gen(v, tauh_mhleg_a, tauh_mhleg_b, tauh_mhleg_c, tauh_mhleg_d);
```

371

```
372 if outswitch==2
```

```
373     gna = GNa .* m .* h;
```

```
374 elseif outswitch==1
```

```
375     gna = GNa .* minf .* hinf;
```

```
376 end
```

377

```
378 if outswitch==2
```

```
379     dm = (minf-m)./taum;
```

```
380     dh = (hinf-h)./tauh;
```

```
381     varargout{1} = dm;
```

```
382     varargout{2} = dh;
```

```
383 elseif outswitch==1
```

```
384     varargout{1} = minf;
```

```
385     varargout{2} = hinf;
386     varargout{3} = taum;
387     varargout{4} = tauh;
388 end
389 end
390
391 function val = hypsec(v, a, b, c, d, e, f)
392 val = a./(exp((v - b)/c) + exp(-(v - d)/e)) + f;
393 end
394
395 function val = gaussian(v, a, b, c, d)
396 val = a.*exp(-((v-b)/c).^2)+ d;
397 end
398
399 function val = sigmoid(v, minf_v50, minf_slope)
400 val = 1./(1+exp((minf_v50-v)./minf_slope));
401 end
402
403 function val = sigmoid_sum(v, a, b, c, d, e, f, g, h)
404 val = a+(b-a)*sigmoid(v,c,d) + f + (e-f)*sigmoid(v,g,h);
405 end
406
407 function val = sigmoid_gauss(v, a, b, c, d, e, f, g, h)
408 val = a + (b-a)*sigmoid(v,c,d) + gaussian(v,e,f,g,h);
409 end
410
411 function val = sigmoid_gen(v, a, b, c, d)
412 val = (a-(a-b)./(1+exp((c-v)/d)));
413 end
414
```